

Theory for the Interdependence of High- T_c Superconductivity and Dynamical Spin Fluctuations

S. Grabowski, J. Schmalian, M. Langer, and K. H. Bennemann

Institut für Theoretische Physik, Freie Universität Berlin, Arnimallee 14, 14195 Berlin, Germany

(June 29, 1995)

The doping dependence of the superconducting state for the 2D one-band Hubbard Hamiltonian is determined. By using an Eliashberg-type theory, we find that the gap function $\Delta_{\mathbf{k}}$ has a $d_{x^2-y^2}$ symmetry in momentum space and T_c becomes maximal for 13 % doping. Since we determine the dynamical excitations directly from real frequency axis calculations, we obtain new structures in the angular resolved density of states related to the occurrence of *shadow states* below T_c . Explaining the anomalous behavior of photoemission and tunneling experiments in the cuprates, we find a strong interplay between d -wave superconductivity and dynamical spin fluctuations.

74.20.Mn, 74.72.-h, 74.25.Jb

Despite important progress, the nature of the superconducting pairing mechanism of the High- T_c -materials is still controversial. Due to their unconventional behavior in the normal as well as in the superconducting state various solely electronic pairing mechanism were proposed [1]. During the last years the symmetry of the superconducting order parameter in momentum space was studied intensively, because it probably holds the key for an understanding of the High- T_c systems and the role of spin fluctuations within the cuprates [2]. Recent angular resolved photoemission (ARPES) experiments and phase sensitive measurements of the gap function [3–7] clearly favor a $d_{x^2-y^2}$ or an anisotropic $s_{x^2+y^2}$ symmetry of the gap in momentum space over an isotropic s -wave scenario. Moreover the maximum of T_c upon doping, the occurrence of an additional dip in the ARPES spectra of $\text{Bi}_2\text{Sr}_2\text{CaCu}_2\text{O}_{8+\delta}$ found by Dessau *et al.* [8] and the dip at $\omega = \pm 3\Delta$ in superconductor-insulator-superconductor (SIS) tunneling measurements [9] are important experiments that may be significant clues for the pairing interaction. In particular, the recent observation of shadows of the Fermi surface (FS) in the paramagnetic state by Aebi *et al.* [10] and their interpretation in terms of short-range antiferromagnetic correlations could be the *Smoking Gun* of a spin fluctuation pairing mechanism. Therefore, the behavior of the shadow states below T_c is of great importance for an understanding of the superconductivity in the High- T_c systems.

Theoretically, a favorite model to study a purely electronically mediated pairing interaction in the CuO_2 plane is the 2D one-band Hubbard Hamiltonian. Recently, it was demonstrated within an Eliashberg-type theory based on the spin-fluctuation mechanism, that there exists a superconducting ground state below $T_c \approx 0.02t$ with a d -wave symmetry of the order parameter [11–13]. Despite these interesting results, the dynamical properties and their relation to the strong antiferromagnetic correlations are far from being understood, because the relevant strong coupling equations were solved on the

imaginary frequency axis which gives no direct access to the dynamical excitation spectrum. A first step to determine the excitation spectrum from a real axis calculation was achieved in an important study by Dahm *et al.* [14].

In this Letter, we present results for the excitation spectrum in the superconducting state and explain the anomalous behavior of the ARPES spectra and tunneling measurements. In addition, we determine the doping dependence of the superconducting state and investigate the interdependence of the superconducting phase and the strong antiferromagnetic correlations within the cuprates. Our theory is based on a strong coupling Eliashberg-type approach for the one-band Hubbard Hamiltonian with nearest neighbor hopping integral $t = 0.25$ eV, bare dispersion $\varepsilon_0(\mathbf{k}) = -2t[\cos(k_x) + \cos(k_y)] - \mu$ with chemical potential μ , and local Coulomb repulsion $U = 4t$. Since we are using our new numerical method [15] for the self consistent summation of all bubble and ladder diagrams (fluctuation exchange approximation, FLEX [16]) on the real frequency axis, we obtain directly the quasi particle excitation spectrum below T_c . The superconducting state is treated in the Nambu formalism where the diagonal and off-diagonal Greens function in the matrix notation can be expanded in terms of the Pauli matrices $\hat{\tau}_i$ ($i = 0, 1, 3$):

$$\hat{G}(\mathbf{k}, \omega) = \frac{\omega Z(\mathbf{k}, \omega) \hat{\tau}_0 - (\varepsilon_0(\mathbf{k}) + \chi(\mathbf{k}, \omega)) \hat{\tau}_3 + \phi(\mathbf{k}, \omega) \hat{\tau}_1}{(\omega Z(\mathbf{k}, \omega))^2 - (\varepsilon_0(\mathbf{k}) + \chi(\mathbf{k}, \omega))^2 - (\phi(\mathbf{k}, \omega))^2}.$$

Here, $\omega(1 - Z(\mathbf{k}, \omega))$ and $\chi(\mathbf{k}, \omega)$ are the diagonal expansion coefficients of the electronic self energy matrix, whereas $\phi(\mathbf{k}, \omega) = \Delta(\mathbf{k}, \omega)Z(\mathbf{k}, \omega)$ is the anomalous self energy and $\Delta(\mathbf{k}, \omega)$ the gap function [17]. Hence, we calculated these functions by solving the Eliashberg equations within the FLEX approximation [18], were the \mathbf{k} and ω dependent pairing interaction and the Greens function $\hat{G}(\mathbf{k}, \omega)$ are calculated self consistently [19].

In Fig. 1 we show the density of states $\rho(\omega)$ in the superconducting phase which is always of $d_{x^2-y^2}$ pairing symmetry for different doping concentrations $x = 1 - n$

and for $T = 63\text{ K}$. Here, n is the occupation number per site. For intermediate doping ($x = 0.14$) a pronounced superconducting gap appears. Due to the d-wave pairing symmetry, states in the gap are clearly visible. For larger doping ($x = 0.18$) the antiferromagnetic correlations are smaller and consequently the pairing interaction and the superconductivity becomes weaker, while for smaller doping ($x = 0.12$) the magnetic correlations are more dominant and we find a sharp increase of the quasi particle scattering. This leads to a loss of metallicity and a weaker superconducting gap. In addition, a pseudogap as a precursor of the Mott-Hubbard splitting becomes visible in $\rho(\omega)$.

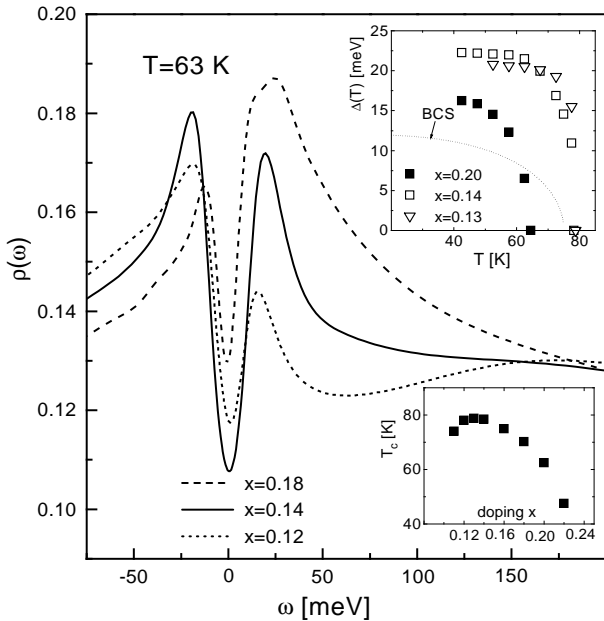


FIG. 1. Density of states $\rho(\omega)$ for three doping concentrations. In the upper inset $\Delta(T)$ is plotted for various doping values. The dotted line is the corresponding BCS curve with an arbitrary chosen $T_c = 75\text{ K}$. In the lower inset the doping dependence of T_c obtained from $\Delta(T_c) = 0$ is shown.

In the upper inset of Fig. 1 we present data for the superconducting gap function $\Delta(T)$ estimated from the distance between the maxima of $\rho(\omega)$ for different doping values. For all doping concentrations the gap opens much faster below T_c than in the corresponding BCS case (dotted lines) and saturates quickly. This is due to the shift of spectral weight in the pairing interaction to higher energies induced by the opening of the superconducting gap and therefore to strong feedback effects [11]. Furthermore, we find in agreement with Raman scattering measurements that the gap opens more rapidly when x is decreased [20]. Interestingly, the tendency that the gap function $\Delta(T)$ saturates at higher values of $\Delta(0)$ when the doping is decreased is reversed between $x = 0.14$ and $x = 0.13$. This behavior reflects the increasing stiffness of the system due to the oncoming antiferromagnetic phase

transition and to the reduction of the charge carrier concentration at the Fermi level resulting from the formation of a pseudogap. Therefore, the interplay between antiferromagnetic correlations and superconductivity leads to an optimal doping concentration. This is demonstrated in the lower inset of Fig. 1, where we present in qualitative agreement with the experimental observation the doping dependence of T_c becoming maximal for $x = 0.13$ and $T_c = 79\text{ K}$.

Recently, we presented corresponding results for the normal state [15] and argued that the observation of shadows of the FS shifted by $\mathbf{Q} = (\pi, \pi)$, by Aebi *et al.* [10] is due to strong magnetic correlations that can be explained in our framework without a staggered antiferromagnetic moment and with a small correlation length of 2.5 lattice spacings. Now, we propose that these shadow states also exist below T_c and that their intensity is even increased compared to the paramagnetic state.

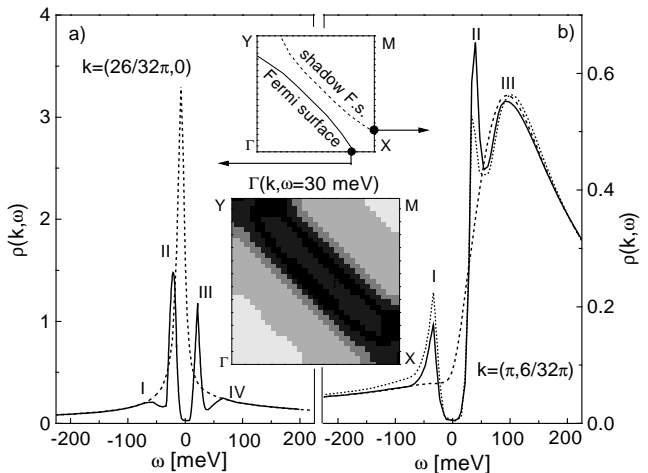


FIG. 2. Spectral density $\rho(\mathbf{k}, \omega)$ for two \mathbf{k} values (see upper inset). (a) $\rho(\mathbf{k}, \omega)$ for $x = 0.16$ and $T = 43\text{ K}$ (solid line) compared with $T = 75\text{ K}$ (dashed line). Note, $T_c(x = 0.16) = 75\text{ K}$. (b) Solid and dashed lines as in (a) and dotted line for $x = 0.14$ and $T = 43\text{ K}$, where $T_c(x = 0.14) = 78.5\text{ K}$. The labeled peaks are discussed in the text. The lower inset shows the \mathbf{k} dependence of the scattering rate $\Gamma(\mathbf{k}, \omega)$ for $\omega = 30\text{ meV}$ where the intensities are represented in a linear grey scale. Note, the largest values of $\Gamma(\mathbf{k}, \omega)$ are along the main FS and its shadow.

In Fig. 2 the spectral density $\rho(\mathbf{k}, \omega)$ for $x = 0.16$ and $T = 43\text{ K}$ is compared with $\rho(\mathbf{k}, \omega)$ in the normal state. In Fig. 2(a) and 2(b), we plot $\rho(\mathbf{k}, \omega)$ for $\mathbf{k} = (26/32\pi, 0)$ close to the FS and for $\mathbf{k} = (\pi, 6/32\pi)$. For the latter momentum one expects in the normal phase the shadow states. As was shown in Ref. [15] these states are clearly visible for smaller doping ($x = 0.12$). In distinction for $x = 0.14$ only a weak maximum and for $x = 0.16$ no shadow states are observable for this \mathbf{k} point above T_c .

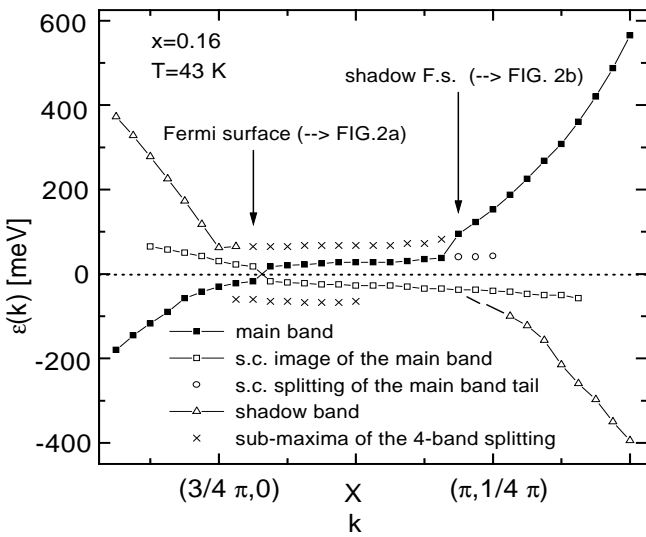


FIG. 3. Quasi particle dispersion below T_c along the high symmetry line $\Gamma \rightarrow X \rightarrow M$ in the neighborhood of the X point. The different symbols represent the dominant contribution to the peaks in $\rho(\mathbf{k}, \omega)$.

In Fig. 2(a), the peak which is slightly below the Fermi level exhibits a superconducting splitting that is almost symmetrical with respect to $\omega = 0$. Besides the main peaks two dips at $\omega \approx \pm 40$ meV are clearly visible. This is related to a strongly enhanced quasi particle decay as will be discussed below.

In Fig. 2(b) the main peak in the normal state is well above the Fermi level. However, a superconducting splitting can be seen below T_c . Pronounced quasi particle decay processes in analogy to Fig. 2(a) and the superconducting splitting of the main band tail for $|\omega| < |\Delta_k|$ lead to the significant dip structure for $\omega > 0$. Most interestingly, these structures can only be found for \mathbf{k} states near the FS and the corresponding shadow states, if $\Delta_k \neq 0$. This results from an anomalous \mathbf{k} dependence of the quasi particle scattering rate $\Gamma(\mathbf{k}, \omega) = \text{Im}(\omega Z(\mathbf{k}, \omega)) / \text{Re}Z(\mathbf{k}, \omega)$ shown in the lower inset of Fig. 2 for $\omega = 30$ meV. Its maxima occur close to the FS but also at the position of its shadow with almost equal intensities leading to a suppression of the spectral weight. We expect this result to be also of importance for the unusual transport properties of the cuprates. In addition, it is highly interesting that the dip structure in Fig. 2(b) is in good agreement with the corresponding ARPES measurements by Dessau *et al.* in the BISCO system [8,21]. By decreasing the doping to $x = 0.14$ the distance between the quasi particle peak in the normal state and the Fermi level increases. Therefore, the spectral weight of the superconducting quasi particles in peak II decreases compared to $x = 0.16$, which one also would

expect for the superconducting image peak I . However, one clearly sees an increase of peak I . In order to show that this observation is due to the formation of superconducting quasi particles within the shadow states, we analyzed the quasi particle dispersion in the superconducting phase.

In Fig. 3, we present this dispersion $\varepsilon(\mathbf{k})$ obtained from the maxima of $\rho(\mathbf{k}, \omega)$. The filled squares indicate the main-band whereas the open squares are due to its superconducting splitting. Note that both exhibit a flat dispersion within a large \mathbf{k} range. This is due to the flat bands in the paramagnetic state and the fact that only the spectral weight below $|\omega| \approx |\Delta_k|$ is splitted in the superconducting phase. Furthermore, the states indicated by open triangles are the shadow states shifted by \mathbf{Q} with respect to the main band. In the paramagnetic state and for $x = 0.16$ these shadow bands are also existent, but their intensities are much weaker. Therefore, a clear amplification of the shadows below T_c occurs. Moreover, we indicate with crosses the maxima caused by the formation of the dip structure. They result, similar to the shadow states, from strong quasi particle decay. For that reason it is tempting to assume that these structures are the continuation of the shadow band structure below T_c for a system with purely dynamical antiferromagnetic correlations. The four band splitting at the FS is due to the fact that the frequency dependence of the quasi particle decay rate of a given band determines that of its superconducting image state. Since both peaks behave symmetrically, we find the significant four band splitting at the FS. Finally, this amplification of the shadow states explains the anomalous doping dependence of the spectral density shown in Fig. 2(b). Although the distance of the peak II and the Fermi level increases upon doping, the crossing point of the shadow states and the Fermi level is shifted towards $\mathbf{k} = (\pi, 6/32\pi)$. The anomalous behavior of peak I results from an increase of its shadow state contribution for smaller doping.

From the effective interaction of the quasi particles, we find that the antiferromagnetic coupling in the superconducting state is even stronger compared to the situation above T_c . Although the magnetic correlation length (≈ 3 lattice spacings) increases by less than one lattice spacings compared to the paramagnetic phase, a clear increase of the effective interaction ($\approx 15\%$) occurs. Due to the retarded coupling of singlet Cooper pairs between nearest neighbor sites, the antiferromagnetic correlations are stabilized on the corresponding time scale. These results indicate not only that the d-wave superconductivity is caused by antiferromagnetic correlations, but that the presence of the superconducting state is also enhancing the short range antiferromagnetic fluctuations. In order to demonstrate further consequences of our theory we also calculated the tunneling conductance for SIN and SIS junctions, because SIS in-plane tunneling measurements exhibit an interesting dip structure at $\omega = \pm 3\Delta$

whose temperature dependence is much stronger compared to the main gap.

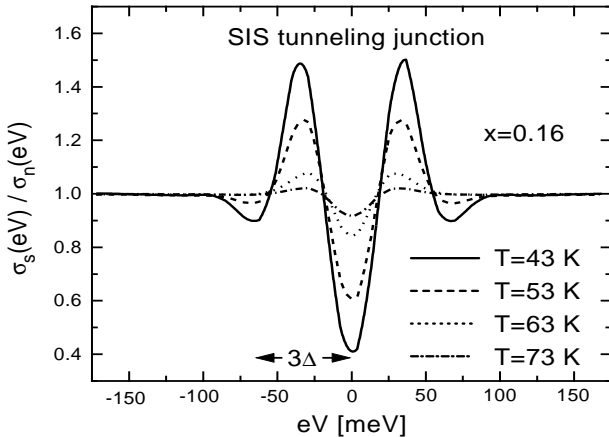


FIG. 4. SIS tunneling conductance $\sigma_s(eV)$ for $x = 0.16$ normalized by the paramagnetic $\sigma_n(eV)$ for different temperatures. Note the strong temperature dependence of the additional dip structure at $\pm 3\Delta$.

In Fig. 4 we present results for the SIS in-plane tunneling conductance $\sigma_s(eV) = dI(eV)/dV$ [9] using

$$I(eV) \propto \int_{-\infty}^{\infty} d\omega \rho(\omega) \rho(\omega + eV) (f(\omega) - f(\omega + eV))$$

for the tunneling current. Here, e is the unity charge, $f(\omega)$ the Fermi function, and V the applied bias voltage. By inserting our self-consistently calculated $\rho(\omega)$, we find an excellent agreement for both the temperature dependence and the position of the dip with the experimental data. Note that in agreement with SIN measurements, no pronounced dip in the corresponding tunneling can be observed (not shown). It is important to point out that our interpretation of the 3Δ dip structure in terms of a strong increase of the scattering rate $\Gamma(\mathbf{k}, \omega)$ at the shadow states is in contrast to the explanation of Ref. [22]. Therein its authors argued that the dip in the SIS measurements is caused by a sudden increase of $\Gamma(\mathbf{k}, \omega)$ at wave vectors $k_x = \pm k_y$ where the gap vanishes.

In conclusion, we calculated the superconducting properties of the 2D Hubbard model. We found that the order parameter has a $d_{x^2-y^2}$ symmetry in momentum space and that T_c is maximal for the doping concentration $x = 0.13$. It was demonstrated for the first time that the shadow states observed by Aebi [10] are still present and even enhanced below T_c . We obtain a four-fold splitting of the quasi particle dispersion at the FS and a dominant dip structure in the spectral density $\rho(\mathbf{k}, \omega)$ next to the shadows of the FS. These new structures are caused by purely dynamical antiferromagnetic spin fluctuations. In view of the recent phenomenological model for a spin fluctuation induced anisotropic s -wave pairing symmetry in bilayers [23] we believe that in our theory a

similar interplay of antiferromagnetic and superconducting excitations occurs for multi-layer systems too. From our spectral density we calculate the in-plane SIS tunneling conductance and demonstrate that the dip in the ARPES and the 3Δ dip in the tunneling characteristics arise for the same physical reason. Therefore, we believe that these important experiments and the observation of shadows of the FS by Aebi *et al.* can be explained within our theory. All this sheds new light on the superconducting pairing mechanism and supports the role of spin fluctuations for the high T_c in the cuprates.

- 1 E. Dagotto, Rev. Mod. Phys. **66**, 763 (1994) and references therein.
- 2 J.R. Schrieffer, Solid State Comm. **92** 1-2, 129 (1994).
- 3 Z.X. Shen, W.E. Spicer, D.M. King, D.S. Dessau, and B.O. Wells, Science **267**, 343 (1995).
- 4 H. Ding *et al.*, Phys. Rev. Lett. **74**, 2784 (1995). M. Randeria, T. Takahashi,
- 5 J.R. Kirtley *et al.*, Nature **373**, 225 (1995).
- 6 D.J. Van Harlingen, Rev. Mod. Phys. **67**, 515 (1995) and references therein.
- 7 A. Mathai *et al.*, Phys. Rev. Lett. **74**, 4523 (1995).
- 8 D.S. Dessau *et al.*, Phys. Rev. Lett. **66**, 2160 (1991).
- 9 D. Mandrus, L. Forro, D. Koller, and Mihaly, Nature **351**, 460 (1991).
- 10 P. Aebi *et al.*, Phys. Rev. Lett. **72**, 2757 (1994).
- 11 P. Monthoux and D.J. Scalapino, Phys. Rev. Lett. **72**, 1874 (1994).
- 12 C.H. Pao and N.E. Bickers, Phys. Rev. Lett. **72**, 1870 (1994).
- 13 P. Monthoux and D. Pines, Phys. Rev. Lett. **69**, 961 (1992).
- 14 T. Dahm and L. Tewordt, Phys. Rev. Lett **74**, 793 (1995).
- 15 M. Langer, J. Schmalian, S. Grabowski, and K.H. Bennemann, preprint.
- 16 N. E. Bickers, D. J. Scalapino, Ann. Phys. (N.Y.) **193**, 206 (1989).
- 17 Details will be published elsewhere.
- 18 Note, a version of the Eliashberg equations on the imaginary axis is given in Ref. [11].
- 19 The calculations are performed on a (64×64) square lattice. We use 4096 equally spaced energy points in the interval $[-30t, 30t]$, leading to a low energy resolution of $0.014t$ (see Ref. [15]).
- 20 T. Staufer, R. Nemetschek, R. Hackl, P. Müller, and H. Veith, Phys. Rev. Lett. **68**, 1069 (1992).
- 21 Note that for the comparison with the experiments one has to perform a particle hole transformation, i.e. an exchange of occupied and unoccupied states and of momenta \mathbf{k} and $\mathbf{k} + \mathbf{Q}$.
- 22 D. Coffey and L. Coffey, Phys. Rev. Lett **70**, 1529 (1993).
- 23 A.I. Liechtenstein, I.I. Mazin, and O.K. Andersen, Phys. Rev. Lett **74**, 2303 (1995).